이학석사 학위논문

Utilizing Space-based Observations of CO_2 and Air Pollutants to Characterize Emissions of Cities

인공위성 관측 자료 기반으로 CO_2 및 대기오염물질의 상관성을 이용한 도시의 배출 특성 분석

2020년 2월

서울대학교 대학원
환경계획학과 환경관리전공
박 하 영

Abstract

Cities account for more than 70% of anthropogenic CO_2 emissions and are a big source of global air pollution. With increased urbanization across the world, cities have been growing rapidly, and intensified human activities and high levels of energy consumption in such areas have led to increased emissions of CO_2 and air pollutants which have a great impact on air quality. We explore the possibility of monitoring urban enhancements of CO_2 using observations from NASA's Orbiting Carbon Observatory-2 (OCO-2) and of air pollutants CO and NO_2 from ESA's Sentinel-5 Precursor TROPOspheric Monitoring Instrument (S-5P TROPOMI) in cities across the globe from December 2018 to March 2019. We use these satellite observations to analyze urban enhancements of ΔXCO_2, ΔXCO, and XNO_2 and enhancement ratios, $\Delta XCO/\Delta XCO_2$ and $XNO_2/\Delta XCO_2$, according to each city to observe the relationship between CO_2 and air pollutants as well as the emission patterns of cities.

Our analysis showed a positive relationship of ΔXCO_2 to ΔXCO and XNO_2, indicating that the increase of CO_2 can lead to an increase in air pollution. However, different patterns were found when cities were grouped into regions. Cities in the Asia region showed the highest concentrations of air pollutants per CO_2, whereas the cities in the American region showed the highest correlation to this positive relationship. Comparisons of $\Delta XCO/\Delta XCO_2$ and $XNO_2/\Delta XCO_2$ show distinct emission patterns

according to different regions of the world. When the $\Delta XCO/\Delta XCO_2$ and $\Delta XNO_2/\Delta XCO_2$ were compared with city population and GDP, it was found that $\Delta XCO/\Delta XCO_2$ had a positive relationship to city population and GDP, indicating that the size of the city and its economy can act as defining factors of air quality. However, when cities were divided into 'developed' and 'developing' based on the economic status of their respective countries, a distinct pattern was found. Developed cities followed the gradual positive relationship of an increase in the ratios of $\Delta XCO/\Delta XCO_2$ and $XNO_2/\Delta XCO_2$ with the increase of city GDP. However, developing cities facing rapid economic development such as Mumbai, Kolkata, and Lahore were seen to break out of the pattern and hold high emission ratios that almost matched that of developed cities. The high emission ratios of $\Delta XCO/\Delta XCO_2$ and $XNO_2/\Delta XCO_2$ in such cities are the results of low combustion efficiency of fossil fuels as well as less stringent pollution control measures.

Finally, we compared our satellite observations of ΔXCO_2, ΔXCO, and XNO_2 to the CAMS Global anthropogenic emissions and found that XNO_2 emission fits best with our observed satellite urban enhancements, while ΔXCO and ΔXCO_2 showed varying patterns within each region. The difference between the emissions dataset and satellite–observed concentrations indicate the influence of transport as well as the uncertainty or underreporting of emissions. The comparison with emissions data also highlighted the importance of geographical features surrounding the city as is the case for Milan, Tehran, and Daegu. These cities are located near mountain ranges or basins where in addition to their high emissions, air

pollution gets trapped within the city as a result of meteorological conditions.

Our study compares CO_2 and air pollutants in cities across the globe using a uniform method with satellites to analyze air quality and different emission patterns that characterize each region. Our findings also suggest that co-benefit can be achieved where the reduction of CO_2 will result in a reduction of air pollutants CO and NO_2, and vice versa. However, as emission patterns vary by region, it is important to apply different reduction policies and methods according to the varying regional emission patterns. Comparisons of CO_2 to air pollutants can give clues as to which is the dominant air pollutant that affects the air quality and what factors and sources can affect their concentration.

Keywords : CO_2, CO, NO_2, urban enhancement, ratios, emission patterns

Student Number : 2018-24455

Table of Contents

Figures.....9

I. Introduction

Despite the importance of cities and the activities of quantifying and understanding anthropogenic emissions and air pollutants over urban areas, such studies are still limited within a few city or country boundaries and lack a global scale analysis that aids in monitoring emissions with sufficient accuracy (Ciais et al., 2014). Cities, which are home to more than half of the global population, account for over 70% of anthropogenic CO_2 emissions and are also culprits of air pollution (Duren and Miller, 2012; Moran et al., 2018, Bares et al., 2018). With global urbanization, cities and urban agglomerations have been growing rapidly and are projected to continue to increase in size and number (Parrish and Zhu, 2009). Intensified human activities and high levels of energy consumption in such areas have led to increased emissions of CO_2 as well as air pollutants which have a great impact on the environment, air quality, and climate change (Molina et al., 2004; Schneider et al., 2015). While they are the biggest emitters of anthropogenic emissions, cities also have great potential to be drivers of global reduction of CO_2 and air pollutants.

CO_2 is a long-lived, chemically stable species that is often co-emitted with other pollutants during anthropogenic activities such as fossil fuel combustion (Wunch et al., 2009). Air pollutants such as CO and NO_2 can be used as a means to disentangle urban enhancements of CO_2 from background concentrations and attribute

its anthropogenic sources (Silva et al., 2017; Bares et al., 2018). CO is produced from combustion processes that use hydrocarbon fuel, and these processes emit both CO and CO_2 depending on the completeness of the combustion (Silva et al., 2013). Due to its chemical lifetime which ranges from a few weeks to a few months, CO is a suitable tracer for pollutant emissions and transport (Clerbaux et al., 2008; Worden et al., 2010). NO_2 is formed and emitted to the atmosphere when fossil fuels are combusted at high temperatures (Richter et al., 2005). NO_2 has a short lifetime and is concentrated near its emission sources, making it advantageous in estimating anthropogenic CO_2 emissions from fossil fuel combustion (Reuter et al., 2014; Kroktov et al., 2016; Hakkarainen et al., 2016; Souri et al., 2016). Atmospheric observations are useful in supporting monitoring activities since CO_2 concentrations in the atmosphere capture and reflect anthropogenic emissions (Kort et al., 2012). Comparing CO_2 together with air pollutants CO and NO_2 allows us to distinguish anthropogenic CO_2 emissions from biogenic influences on CO_2 concentrations. Moreover, it also enables the distinction and characterization of emission sources and their link to air quality.

Space-based measurements of urban enhancements of CO_2 and air pollutant observations have been increasingly used for atmospheric monitoring because of the advantage of satellites which provide a continuous dense spatial sampling with a global coverage, even covering areas where air quality monitoring stations are either sparse or not available (Baker et al., 2010; Schneider et al., 2015;

Labzovskii et al., 2019). However, there are major challenges with atmospheric observations especially of CO_2 concentrations within cities considering the long lifetime of CO_2 and seasonal impacts of biospheric fluxes which complicate the disentangling of anthropogenic and biospheric signals, while atmospheric transport obfuscates source attribution (Kort et al., 2012; Briber et al., 2013; Hutyra et al., 2014; Hakkarainen et al., 2016).

Many studies have been carried out using satellite observations to analyze urban enhancements of anthropogenic CO_2 concentrations together with CO and NO_2. Hakkarainen et al. (2019) used satellite-based observations of NO_2 to estimate the emissions and spatio-temporal variability of CO_2 from point sources, while Berezin et al. (2013) used satellite measurements of NO_2 to verify CO_2 emissions from fossil fuel combustion. Silva et al. (2013) took retrievals of CO from MOPITT and CO_2 from the GOSAT/ACOS satellite to analyze the CO_2/CO enhancement ratios ($\Delta CO_2/\Delta CO$) over megacities. The observed $\Delta CO_2/\Delta CO$ showed a general pattern in combustion activity as well as the "developed" and "developing" statuses of megacities. In a subsequent study, Silva et al. (2017) used satellite observations of CO, NO_2, and CO_2 across 46 megacities obtained from GOSAT/ACOS, MOPITT, and OMI/DOMINO, respectively, and demonstrated that space-based observations of enhancement patterns can distinguish combustion source characteristics such as combustion activity and efficiency in a regional scale. Reuter et al. (2019) analyzed co-located regional enhancements of CO_2 and NO_2 from the OCO-2 and Sentinel-5P

TROPOMI satellites, respectively, and estimated the cross-sectional fluxes of CO_2 plumes in small scale emissions to demonstrate that NO_2 can be applied as a tracer of recently emitted CO_2 to identify the source of the XCO_2 enhancements in urban areas and constrain plume structure.

However, there is still a lack of studies using CO_2 and air pollutants CO and NO_2 as a means to observe air quality. Also, most studies only focus on small-scaled areas or a specific city or region, which allows for extensive analysis but lack a global comparison. Moreover, synergies using different space-based measurements are needed to better understand the relationship between CO_2 concentrations and air pollutants in cities and utilize the information to distinguish regional emission characteristics (Silva et al., 2017; Bares et al., 2018).

In this study, we observe the relationships between urban enhancements of CO_2 and air pollutants CO and NO_2 using satellite observations from NASA's Orbiting Carbon Observatory-2 (OCO-2) and ESA's Sentinel-5 Precursor TROPOspheric Monitoring Instrument (S5-P TROPOMI). We examine whether high concentrations of CO_2 lead to a high concentration in air pollutants, signifying bad air quality. We also demonstrate how the relationships of CO_2 and air pollutants CO and NO_2 can show similarities and differences in characteristics of anthropogenic emission patterns of cities across the globe. We focus our analysis on the winter season from December 2018 to March 2019 as this

period corresponds to the datasets available from both satellites used in this study.

II. Methodology

2.1 OCO-2 XCO_2 observations

The Orbiting Carbon Observatory-2 (OCO-2) was launched in July 2014 aiming to continue and improve the column-averaged CO_2 dry air mole fraction (XCO_2) observations from space. It is the first NASA satellite to measure the sources and sinks of CO_2 with high accuracy, resolution, and coverage over the globe. It has a three-band spectrometer which measures the absorption by CO_2 and O_2 in reflected sunlight in three independent wavelength bands: the O_2 A-band at around 0.765 μm, the weak CO_2 band at around 1.61 μm, and the strong CO_2 band at around 2.06 μm (Crisp et al., 2008; Eldering et al., 2017a). OCO-2 is part of the A-train constellation and flies in a sun-synchronous orbit and its ascending nodes cross the equator at 13:36 local time. It runs in a push-broom-like fashion along its track with a spatial resolution of 1.29 km x 2.25 km at ground and has eight footprints that are each 1.25 km in width (Crisp et al., 2017; Eldering et al., 2017b). We use NASA's operational bias-corrected OCO-2 L2 Lite XCO_2 product v9 which is the dataset that has been rigorously pre- and post-

filtered for potentially unreliable soundings including the retrievals contaminated with cloud and aerosols (O' Dell et al., 2018).

2.2 S-5P TROPOMI XCO, XNO_2 observations

The TROPOspheric Monitoring Instrument (TROPOMI) was launched on the Copernicus Sentinel-5 Precursor satellite in October 2017. The instrument is a sun-synchronous nadir-looking grating spectrometer that runs in a push-broom way and performs measurements of the solar light reflected by the Earth's atmosphere in the UV-VIS (270-495 nm), NIR (710-775 nm), and SWIR (2305-2385 nm) spectral domain (Veefkind et al., 2012). The advantage of this instrument is the 2600 km swath which provides daily global coverage in combination with high spatial resolution of the measurements of CO (7 km x 7 km, SWIR) and NO_2 (7 km x 3.5 km, UVN) and a high signal-to-noise ratio, enabling daily observations of air quality and detection of CO and NO_2 pollution over cities and industrial areas using single orbit overpasses (Doornink et al., 2014; Borsdorff et al., 2019).

2.3 MODIS urban land cover pixels

In order to obtain satellite observations over urban areas, we used the Moderate Resolution Imaging Spectroradiometer (MODIS) global map of urban extent with a spatial resolution of 500

m. The urban pixels are determined using the decision tree algorithm and an ensemble of classification techniques (Schneider et al., 2009). The MODIS urban extent map was accessed online (https://www.naturalearthdata.com/downloads/10m-cultural-vectors/10m-urban-area/). We used MODIS urban pixels to delineate the boundaries of cities to disregard administrative boundaries and instead define the term "cities" as numerically quantified units of urban areas. We used satellite observations over large cities with an area > 1000 km^2 in order to obtain as many observations as possible considering the short period of the study in addition to the infrequent OCO-2 visits to cities. A total of 133 cities that met this criterion were analyzed in this study. The official name of the urban agglomeration or the largest city corresponding to the urban area was used to label each unit.

2.4 CAMS Global anthropogenic emissions

The Copernicus Atmospheric Monitoring Service (CAMS) Global anthropogenic emissions is an inventory dataset developed by the European Centre for Medium-Range Weather Forecasts (ECMWF) as part of the implementation of Copernicus, the European Union's Earth observation programme. The CAMS Global anthropogenic emissions data is based on a combination of the CEDS and EDGAR v4.3.1 historical data. The emissions dataset has

a global coverage with a spatial resolution of 0.1 x 0.1 degrees and a temporal coverage for the year 2000 to 2019. The CAMS Global anthropogenic emissions cover 36 anthropogenic gas parameters from 15 different sectors and the emissions are provided as monthly averages (Granier et al., 2019).

2.5 Calculation of urban enhancements

Urban enhancements, especially enhancements of CO_2, of individual anthropogenic point sources are usually small compared to the background concentration and its natural variability. CO_2 has a long atmospheric lifetime and a comparably large background concentration that adds up to almost 410 ppm and varies only by a small percentage from pole-to-pole (Hakkarainen et al., 2019). Therefore, it is necessary to remove the background concentrations and seasonal variability to identify emission areas as well as to map together short-lived pollutants like CO and NO_2 with space-based CO_2 measurements. Using anomaly calculations by taking the difference between the "contaminated" and "clean" gradient allows us to remove the seasonal variability and detrend CO_2 observations from background concentrations (Kort et al., 2012; Hakkarainen et al., 2016). In this study, we used the methodology of *Labzovskii et al.* (2019) and applied it to our urban anomaly calculation. The anomaly calculation which extracts urban enhancements is expressed as the following equation.

$$\Delta Xobs = Xobs_{urb} - Xobs_{bck} \quad (1.0)$$

Urban enhancement (urban anomaly, ΔXobs) is defined as the difference between the individual satellite observation value measured by OCO−2 and TROPOMI and their respective background concentrations. First, the observations of CO_2, CO, and NO_2 falling over cities were classified as "urban" soundings ($Xobs_{urb}$). The XCO_{urb} and XNO_{2urb} soundings were then each collocated to match the XCO_{2urb} soundings over each city. All the soundings over land that do not fall over the cities covered in our study or other MODIS urban pixels are assigned as "rural" soundings ($Xobs_{rur}$). We created a buffer area of 10 km from the boundaries of the cities in our study and did not use any rural soundings falling within that area in our analysis to avoid any nearby influence from urban areas in our background concentrations. Next, we set a background box of ~500,000 km^2 around the center point of each city of our study. The daily median $Xobs_{rur}$ soundings falling within the background boxes of each city are defined as the background concentrations ($Xobs_{bck}$). We then subtracted $Xobs_{bck}$ from each $Xobs_{urb}$ soundings of the same day to calculate the urban enhancements (ΔXobs) of cities within the period of study. Considering the short lifetime of NO_2 and the fact that NO_2 sources within urban areas are mainly anthropogenic, we used the XNO_{2urb} soundings without calculating the urban enhancements of NO_2 in our study. We show an example of urban area delineation and anomaly calculation in Figure 1.

We included as many cities as possible in our sample for analysis but still set a threshold to filter out any cities with < 10 XCO_2 observations within the city and < 20 XCO_{2rur} observations within each respective daily background box during the four months of the study. A total of 65 cities were left that passed the threshold test and were used in our study. The distribution of all the observations over cities and calculated anomalies are shown in Figure 2. The mean and median concentrations of XCO and XCO_2 show a high probability of urban enhancements when calculated as anomalies. Whereas for XNO_2, with its homogenous characteristic over urban areas and its short lifetime (Beirle et al., 2003), urban enhancements are better captured without considering its background concentration and calculating the anomalies.

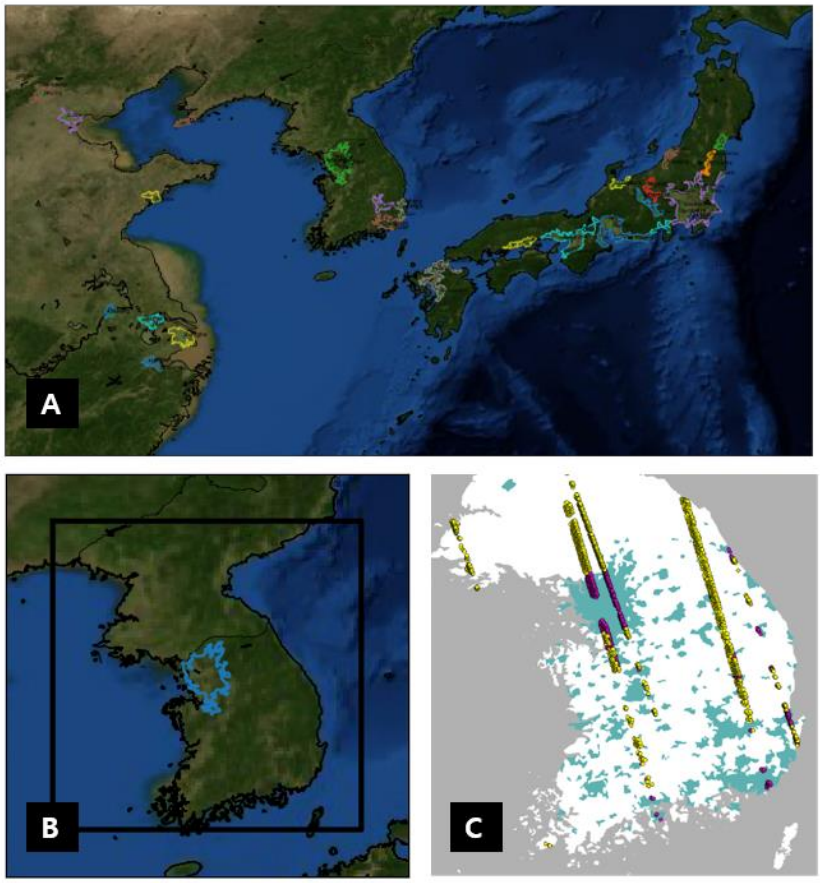

Figure 1. (a) A sample of cities with area > 1000 km^2 delineated with MODIS urban pixels in East Asia. (b) Background box of area ~500,000 km^2 shown as a black frame. (c) Satellite observations of $Xobs_{urb}$ of Seoul (magenta) and $Xobs_{rur}$ (yellow) falling within the background box are used as $Xobs_{bck}$ to calculate $\Delta Xobs$.

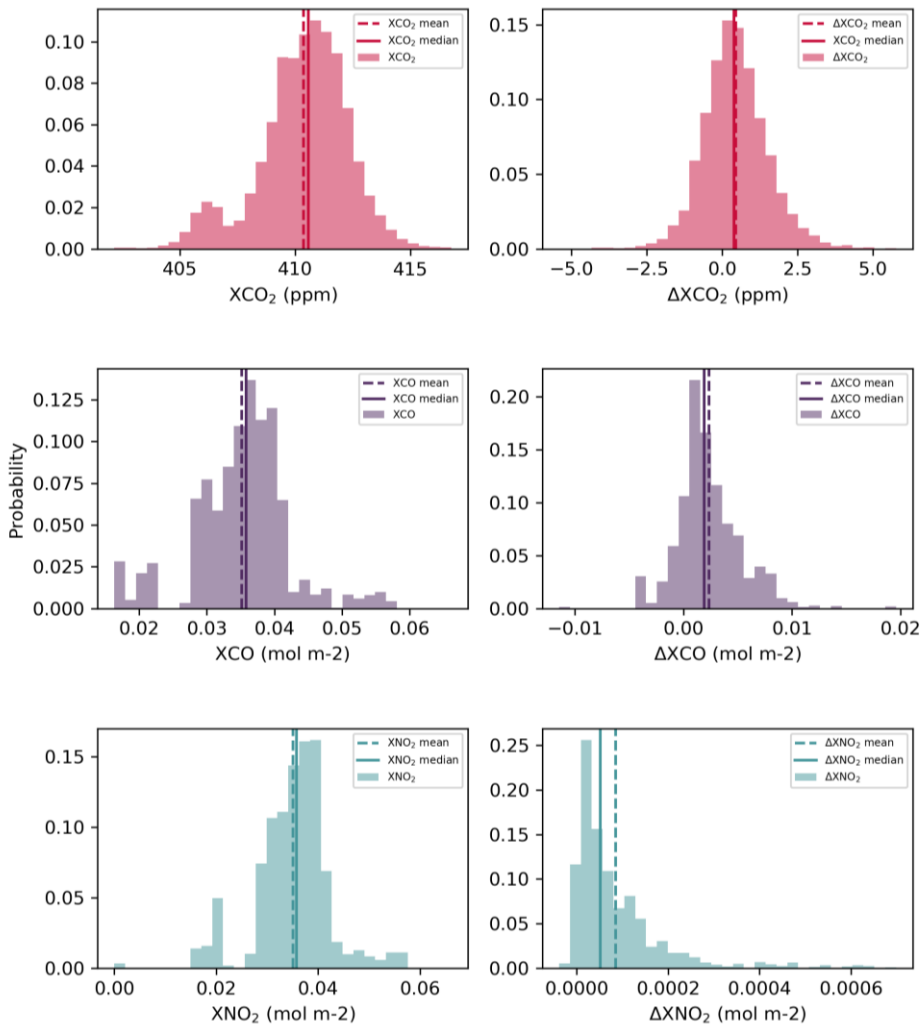

Figure 2. Probability density function of XCO_2, XCO, XNO_2 and ΔXCO_2, ΔXCO, ΔXNO_2.

III. Results

3.1 Comparison of mean ΔXCO and XNO_2 to ΔXCO_2 of cities

The mean ΔXCO_2 was compared to the mean ΔXCO and mean XNO_2, respectively. In the global analysis shown in Figure 3, both mean ΔXCO and XNO_2 show a positive relationship with mean ΔXCO_2, implying that cities with higher concentrations of CO_2 tend to have higher concentrations of air pollutants. As can be seen in Figure 3, increased anthropogenic activities and use of energy lead to an increased emission of pollutants, and most of the intense anthropogenic emissions are related to large cities. However, within the global positive relationship, cities show different patterns when grouped into their respective regions of the world. For careful examination between regions, we clustered the cities of our study into three main regions for comparison – Asia, North America, and Europe. We excluded cities in the Southern Hemisphere in our regional analysis because of the contrast in seasons.

3.1.1. Comparison of mean ΔXCO and mean ΔXCO_2

In the comparison between mean ΔXCO and ΔXCO_2, Asian cities have the highest ΔXCO and ΔXCO_2 concentrations overall, with cities such as Tehran, Isfahan, and Peshawar showing especially high ΔXCO and ΔXCO_2 concentrations. On the other hand, cities in Europe and North America generally have a lower concentration of ΔXCO compared to their high ΔXCO_2 concentrations. For example, comparing the cities from each region which have similarly high concentrations of mean ΔXCO_2, Peshawar (1.31 ppm), Los Angeles (1.25 ppm), and Frankfurt (1.48 ppm), the order of highest to lowest concentration of mean ΔXCO is Peshawar (0.0069 mol m−2), Los Angeles (0.0044 mol m−2), and Frankfurt (0.0038 mol m−2). CO is a hazardous pollutant emitted from anthropogenic sources such as vehicles, industry, and domestic heating. It is produced as a by−product together with CO_2 during various combustion processes using hydrocarbon fuel, and more CO is produced depending on the efficiency and completeness of the combustion (Turnbull et al., 2011; Silva et al. 2017).

The higher concentrations of ΔXCO per ΔXCO_2 concentrations of Asian cities can be explained by the higher usage of older car fleets and dependency on fossil fuels such as coal−fired power plants (Clerbaux et al., 2008). High concentrations of ΔXCO per ΔXCO_2 in European and North American cities may be related to large power facilities and increased use of cars and home

heating during winter. However, in Figure 4, cities in Europe and North America have a lower ΔXCO per ΔXCO_2 than cities in Asia, which can be attributed to the lower dependency on coal and the gradual shift to using energy from natural gas and renewables. (Bölük & Mert, 2014; Koplitz et al., 2017)

CO is not only emitted from anthropogenic sources, but also from natural sources like fires, whether or not it is initiated by humans. Therefore, the sources of CO vary in different parts of the world and in different seasons. For example, in our global analysis, Rio de Janeiro has a negative mean ΔXCO_2, which conveys that this city acts as a sink for CO_2. Contrastingly, the concentration of mean ΔXCO is extremely high as a result of the seasonal burning of the Amazon forest in Brazil which happens during the dry season from June to December (Crutzen & Andreae, 1990).

3.1.2. Comparison of mean XNO_2 and mean ΔXCO_2

The comparison of mean XNO_2 and ΔXCO_2 also shows a global positive relationship, indicating that cities with high emissions of anthropogenic CO_2 also have high emissions of NO_2. However, within this global positive relationship, varying regional patterns exist. NO_2 is an air pollutant in the troposphere that is harmful to human health as it produces ozone and acid deposition during a catalytic chain reaction. Its main source is the emission of nitrogen

monoxide from the fossil fuel itself during anthropogenic combustion and also from the decomposition of N_2 in the air at high temperatures (Hillboll et al., 2013; Silva et al., 2017).

In the regional analysis, all three regions have a positive relationship between the mean XNO_2 and mean ΔXCO_2. As with the comparison between mean ΔXCO and mean ΔXCO_2, Asian cities showed a higher concentration of XNO_2 per ΔXCO_2 compared to North American cities. The high concentration of NO_2 pollution in this region can be linked to the rapid economic growth of cities mainly in South Asia and China which is generally coupled with a large growth in energy consumption. These cities are also densely populated often with large increases in motor vehicles and congestion, resulting in idling vehicles and high NO_2 emissions (Hassler et al., 2016). Also, in addition to agricultural activities and continued use of biomass fuel, the growth of industrial activities such as the expansion of oil refining complexes and thermal power plants have largely resulted in high concentrations of NO_2 (Tariq & Ali, 2015; Hassler et al., 2016).

Cities in the North American and European regions show a lower concentration of XNO_2 per ΔXCO_2 despite higher concentrations of ΔXCO_2 compared to cities in the Asian region. This can be attributed to a combination of the implementation of emission control devices on thermal power plants, the shutting off of old and inefficient plants, stricter vehicle emission standards, and other various environmental regulations and initiatives that have led to a decrease in NO_2 (Duncan et al., 2016). However,

concentrations of NO_2 remain high in large cities such as Chicago, Paris, and Manchester. Regardless of the advancement in emission technology, the large number of on-road motor vehicles and traffic congestion that is ubiquitous in many cities result in high emissions of air pollutants (Hassler et al., 2016).

Moreover, in this comparison of mean XNO_2 to mean ΔXCO_2, cities like Tehran and Milan show extremely high enhancements of XNO_2 compared to their ΔXCO_2 concentrations. In the case of Tehran, which has the highest mean XNO_2 (0.00039 mol m-2), 80% of the city's pollution is due to cars. Not only does the city have heavy traffic and large amounts of old and aging cars, but also vehicles are using low-quality gasoline (Hassani & Hosseini, 2016). With international sanctions imposed on Iran, the government has allowed petrochemical refineries to manufacture gasoline that does not meet proper standards (Asadollah-Fardi, 2008).

In addition, geographical features surrounding the city greatly affect urban pollution. Factors that pollute the air in Tehran are heightened by the Alborz mountain range which blocks wind flow and causes thermal inversion that traps the pollution in the city (Atash, 2007). This is also the case for Milan. As seen in Figure 4, on top of its high ΔXCO_2, Milan has high concentrations of XNO_2 and ΔXCO. Much of the pollution sourced from within the city through vehicles and domestic heating is exacerbated by the nearby Po Valley where the Alps and Apennines continue to trap air pollution (Seibert et al., 1998; Bigi et al., 2012).

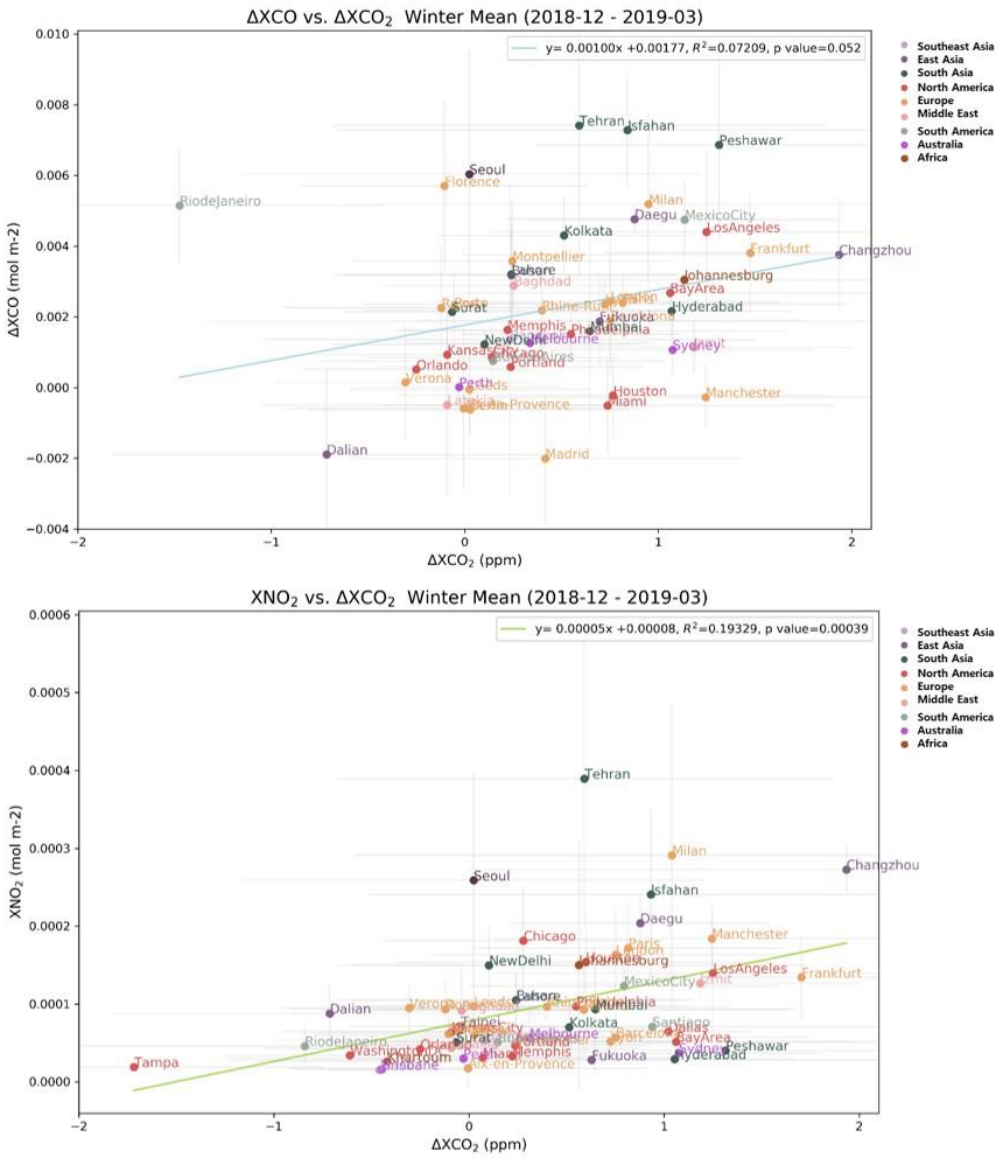

Figure 3. Comparison of mean ΔXCO and ΔXCO_2 concentrations and mean XNO_2 and ΔXCO_2 concentrations of all cities during the winter of December 2018 to March 2019. Each city is associated with a color representing the region it is a part of. Grey lines represent the error of one standard deviation of mean calculation.

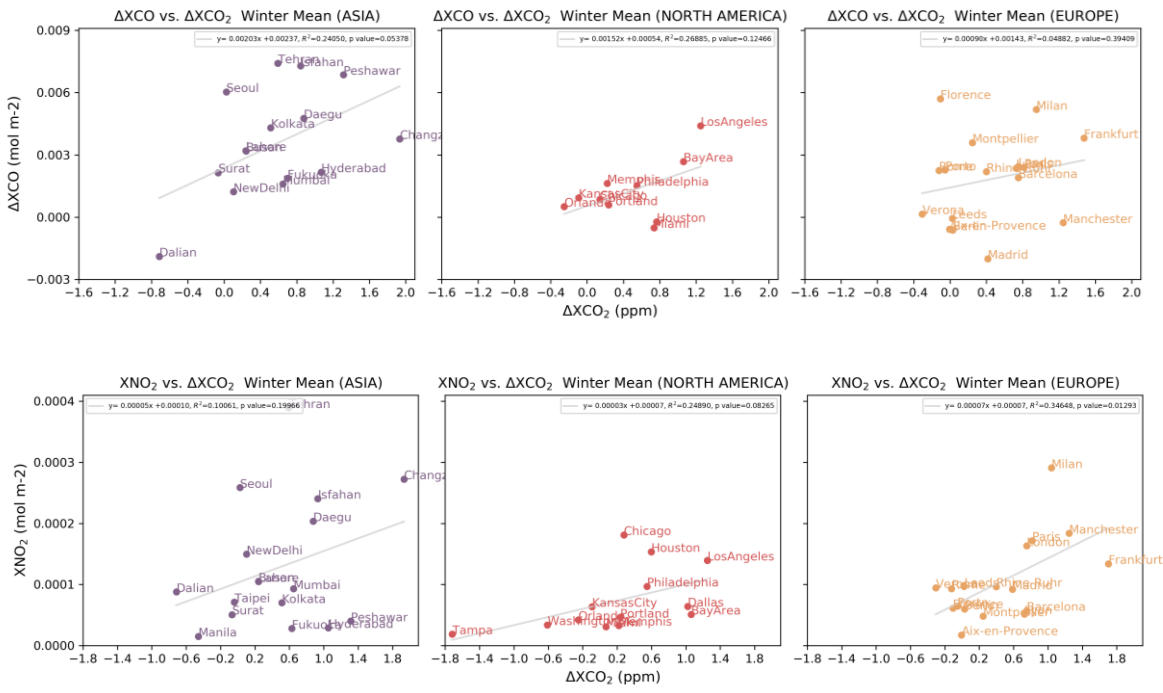

Figure 4. Comparison of mean ΔXCO and ΔXCO_2 concentrations and mean XNO_2 and ΔXCO_2 concentrations of all cities grouped into regions.

3.2 $\Delta XCO/\Delta XCO_2$ and $XNO_2/\Delta XCO_2$ ratios of cities

3.2.1 $\Delta XCO/\Delta XCO_2$ and $XNO_2/\Delta XCO_2$ ratios

We performed regression analyses of ΔXCO_2 with ΔXCO and XNO_2 for each city to calculate $\Delta XCO/\Delta XCO_2$ and $XNO_2/\Delta XCO_2$ using the method of *Silva et al.* 2013. The ratio of ΔXCO and XNO_2 to ΔXCO_2 can be used to identify characteristics of the air quality, as the ratio signifies how much air pollutant per emission of CO_2 is in the atmosphere which has been captured by the satellite signals. Figure 5 shows that Asia has the highest mean $\Delta XCO/\Delta XCO_2$ (0.00064) out of the three regions, while North America has the lowest mean $\Delta XCO/\Delta XCO_2$ (0.00032). Likewise, for the ratio of $XNO_2/\Delta XCO_2$, Asia has the highest mean $XNO_2/\Delta XCO_2$ (0.000021) while North America has the lowest mean $XNO_2/\Delta XCO_2$ (0.000009). In addition to the high mean ratios, cities in Asia have a wider range of ratio values compared to the cities in the North American and European regions.

We then compared the ratios individually with each of its components. Figure 6 comprises of a comparison of $\Delta XCO/\Delta XCO_2$ to ΔXCO_2 and ΔXCO, and a comparison of $XNO_2/\Delta XCO_2$ to ΔXCO_2 and XNO_2. As seen in Figure 6, although ΔXCO_2 plays a significant role, $\Delta XCO/\Delta XCO_2$ and $XNO_2/\Delta XCO_2$ are mainly influenced by the concentration of ΔXCO and XNO, which ultimately determines the air quality within the city.

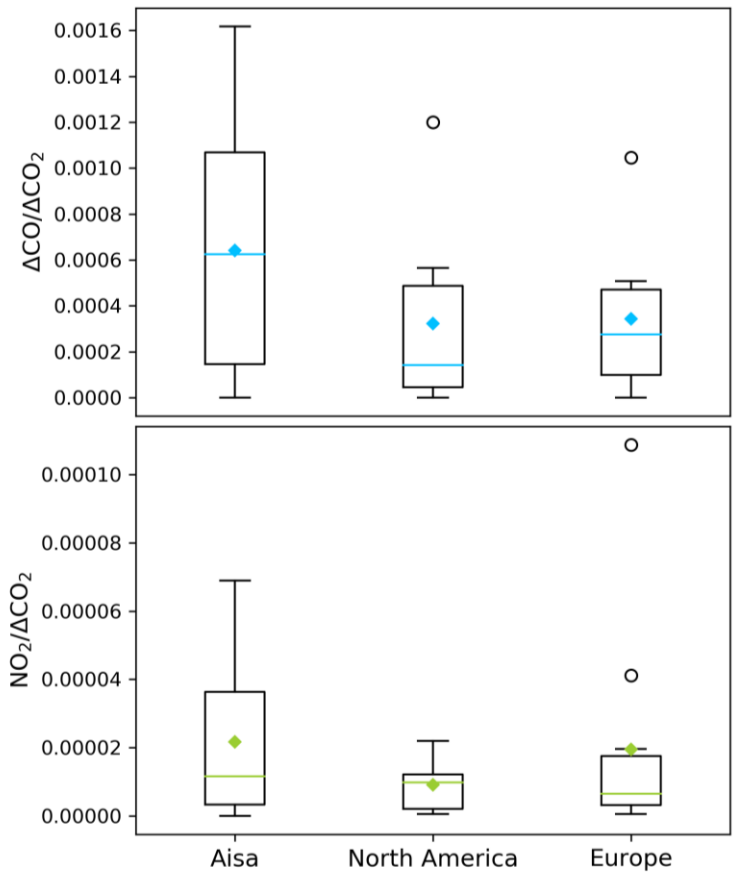

Figure 5. Box plot of $\Delta XCO/\Delta XCO_2$ (top) and $XNO_2/\Delta XCO_2$ (bottom) ratios of cities grouped into regions Asia, North America, and Europe. The diamond represents the mean value and the line represents the median value.

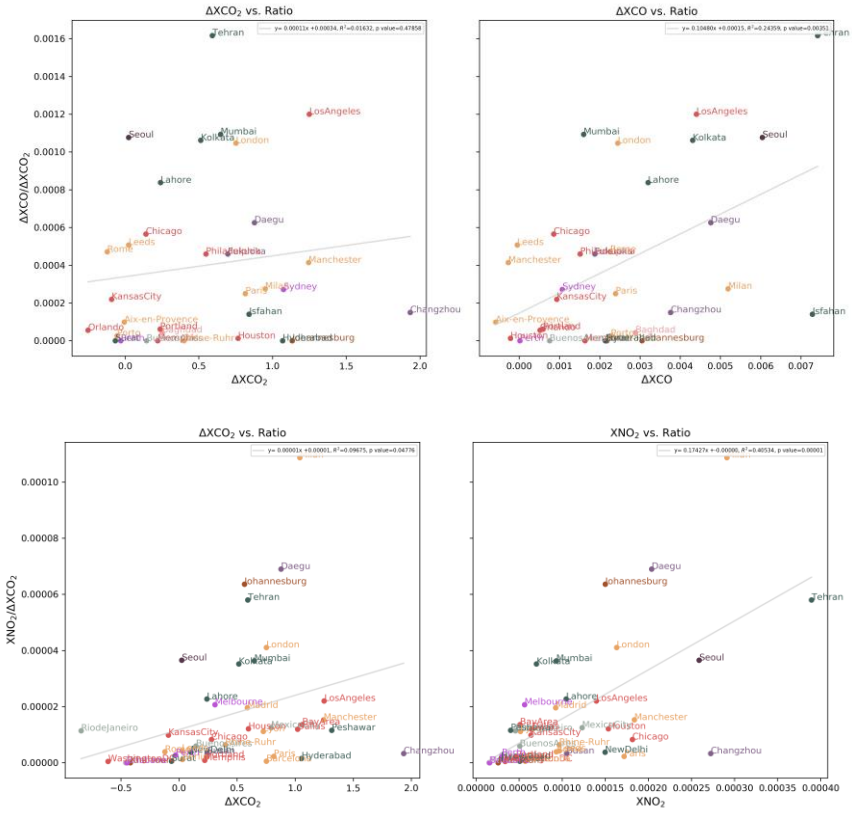

Figure 6. Comparison of $\Delta XCO/\Delta XCO_2$ vs. ΔXCO_2 and ΔXCO (top), and comparison of $XNO_2/\Delta XCO_2$ vs. XNO_2 and ΔXCO_2 (bottom).

3.2.2 Comparison of $\Delta XCO/\Delta XCO_2$ and $XNO_2/\Delta XCO_2$ to population & GDP of cities

To further analyze what other anthropogenic factors contribute to the ratios, a similar comparison was made with $\Delta XCO/\Delta XCO_2$ and $XNO_2/\Delta XCO_2$ to city population and total city Gross Domestic Product (GDP). Population relates to the size of a city, whereas GDP is an indicator of the economic size and economic activity within the city. Data of city population were derived from the 2015 data of OECD Statistics and NASA SEDAC UN WPP-Adjusted Population Count, v4.11. The total city GDP data were obtained from the OECD Statistics and national databases of the cities.

Figure 7 shows that $\Delta XCO/\Delta XCO_2$ has a positive relationship to population and GDP. This pattern is also shown in all three regions. The bigger the city size with a large number of people, the more anthropogenic activities happen within the city, such as heavy on-road traffic and increased use of home heating, ultimately leading to higher ratios of $\Delta XCO/\Delta XCO_2$. The comparison of $\Delta XCO/\Delta XCO_2$ to GDP also shows a positive relationship. High $\Delta XCO/\Delta XCO_2$ ratios of cities with high GDP can also be explained with similar explanations with that of the relationship between $\Delta XCO/\Delta XCO_2$ and population. As the economic size and activity of the city increases, more CO per CO_2 is emitted into the atmosphere for reasons of increased traffic and ongoing industrial activity such as fossil fuel combustion in factories.

Despite the overall positive relationship of $\Delta XCO/\Delta XCO_2$ to population and GDP, different regional trends are found. As seen in Figure 8, $\Delta XCO/\Delta XCO_2$ of cities in North America show the highest

positive correlation to population, with cities in Asia placing second. In the comparison of $\Delta XCO/\Delta XCO_2$ to GDP, cities in North America showed the highest positive correlation. On the other end, Asian cities located in the south of the region such as Mumbai, Tehran, Kolkata, and Lahore have a high $\Delta XCO/\Delta XCO_2$ despite their low GDP.

There were no significant patterns of $XNO_2/\Delta XCO_2$ to city population and GDP globally. This could be due to consistent outliers with high $XNO_2/\Delta XCO_2$ such as Milan, Tehran, and Daegu. Regionally, only North America showed a significant correlation of $XNO_2/\Delta XCO_2$ to population and GDP as shown in Figure 8. In Europe, aside from Milan, London has the highest $XNO_2/\Delta XCO_2$ (0.000041). London has consistently ranked as the European city with the highest average annual NO_2 concentration, exceeding both UK and EU guidelines. High concentrations of NO_2 can also be attributed to the large number of vehicles that pass the test for legal pollution level limits, yet emit much more NO_2 when driven on roads (Rhys-Tyler et al., 2011).

Overall, cities in the North American region show a clear positive relationship and have the highest correlation of $\Delta XCO/\Delta XCO_2$ and $XNO_2/\Delta XCO_2$ to city population and GDP among the three regions. Among the two ratios, for cities in North America, the $\Delta XCO/\Delta XCO_2$ ratio showed the best correlation with population and GDP (R^2 = 0.85 and R^2 = 0.82, respectively). With the sample of cities in the North American region in our study, this means that as city size and economy increases, there is also a pattern of increase in CO and NO_2 concentrations that result in air pollution. In this case, when cities in North America reduce CO_2 emissions, they can also obtain a co-benefit of a reduction in air pollutants, hence achieving better air quality. This co-benefit would also be valid

when reducing air pollutants, which would lead to a reduction in CO_2 concentrations.

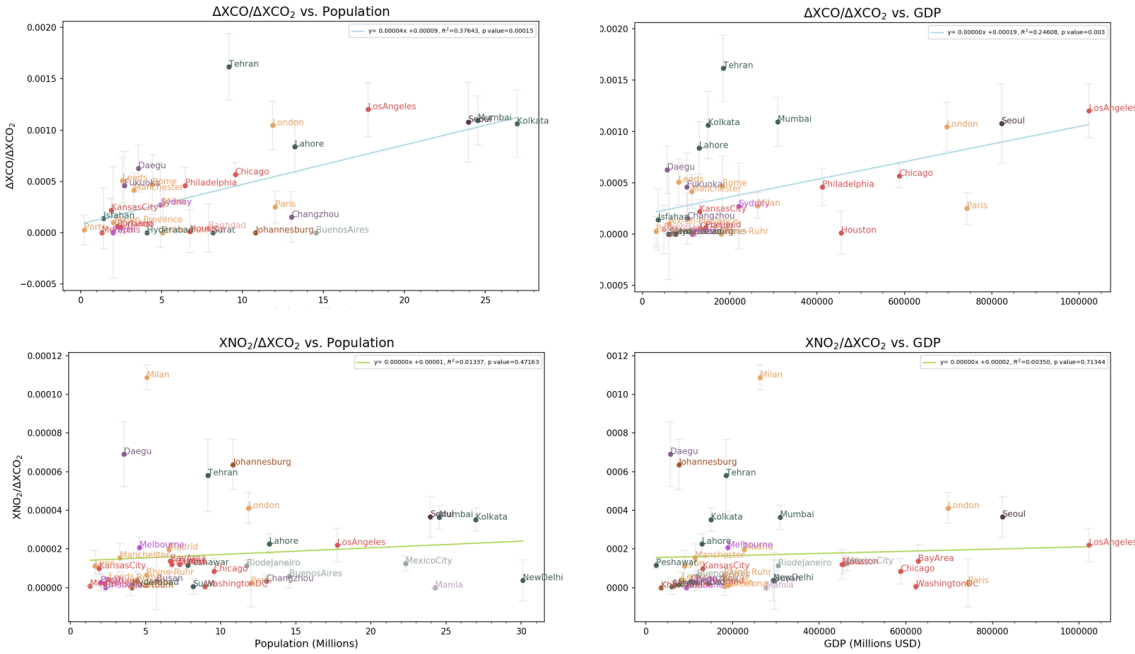

Figure 7. $\Delta XCO/\Delta XCO_2$ and $XNO_2/\Delta XCO_2$ of all cities are compared to population and GDP

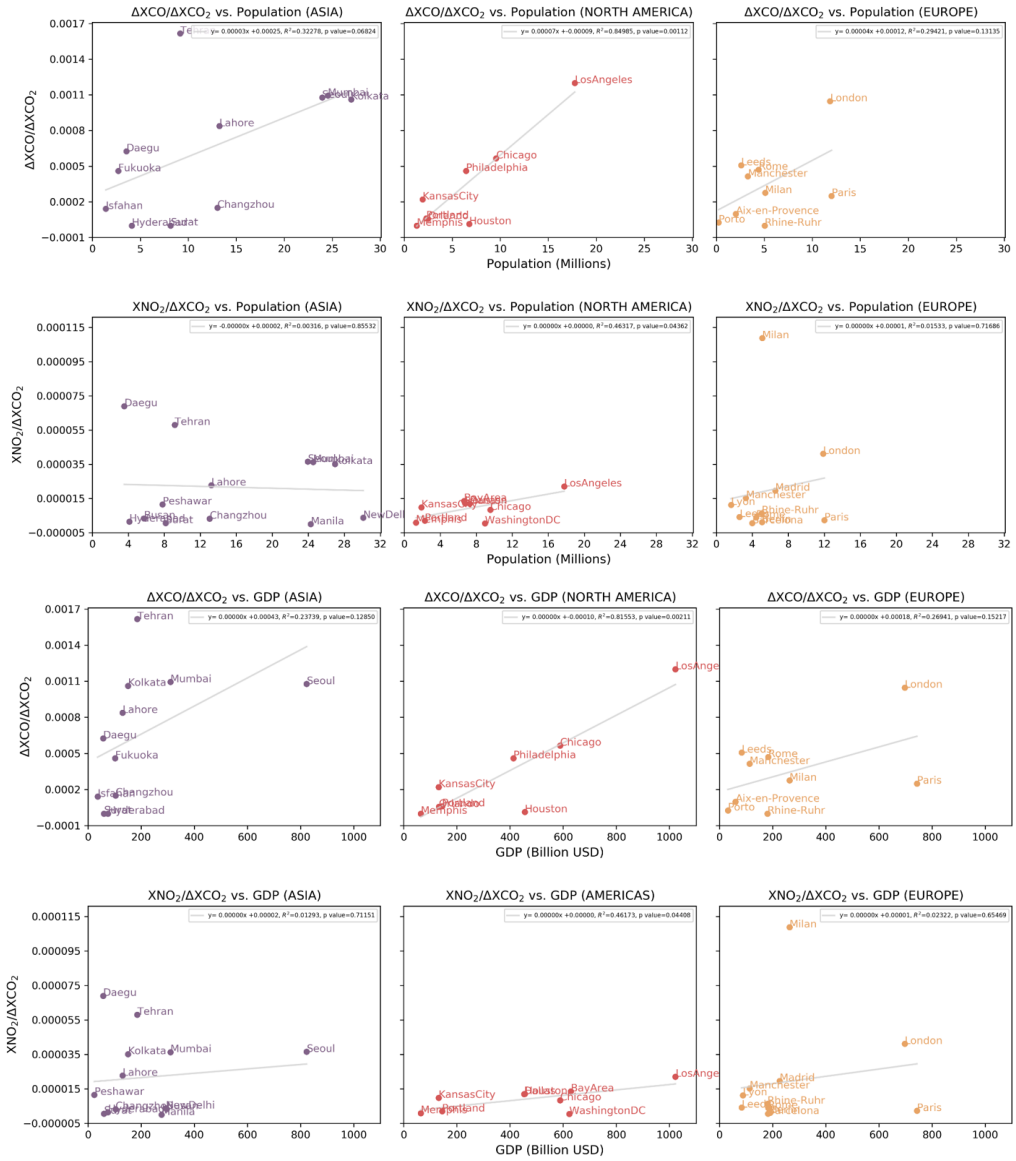

Figure 8. Cities are grouped into regions and $\Delta XCO/\Delta XCO_2$ and $XNO_2/\Delta XCO_2$ are compared to population and GDP.

3.2.3 Comparison of $\Delta XCO/\Delta XCO_2$ and $XNO_2/\Delta XCO_2$ to GDP of developed and developing cities

We furthered our analysis on the comparison of the $\Delta XCO/\Delta XCO_2$ and $XNO_2/\Delta XCO_2$ emission ratios with city GDP. We divided the cities of the three regions into 'developed' and 'developing' cities according to the economic status of their respective countries. As presented in Figure 9, the developed and developing cities show a contrast in pattern. Developed cities show higher ratios of both $\Delta XCO/\Delta XCO_2$ and $XNO_2/\Delta XCO_2$, whereas developing cities have lower ratios of both of $\Delta XCO/\Delta XCO_2$ and $XNO_2/\Delta XCO_2$. However, the pattern can be seen to be broken with cities such as Mumbai, Kolkata, Lahore, and Tehran, which are cities that are undergoing rapid economic development. Despite their low GDP, these cities show $\Delta XCO/\Delta XCO_2$ and $XNO_2/\Delta XCO_2$ ratios that match or are even higher than that of developed cities.

This difference between developed and developing cities can be explained through lower fossil fuel combustion efficiency in the cities of developing countries in addition to less strict pollution control measures. In this case, the emission ratios of developing cities can be explained as being inversely proportional to fossil fuel combustion efficiency, which signifies that the higher values correspond to lower combustion efficiency and lower values correspond to higher combustion efficiency.

Within cities, the biggest contribution to air pollution is cars and their fuel type. NO_2 and CO are both co-emitted with CO_2 from cars. Generally, diesel fuel is observed to have a relatively higher NO_2 emission ratio, whereas cars using natural gas and gasoline for fuel release less NO_2 but more CO (Bares et al., 2018). We made

the same comparison between ratios of $\Delta XCO/\Delta XCO_2$ and $XNO_2/\Delta XCO_2$ to the number of vehicles within the city. The data of the number of vehicles in use in each city for the year 2015 were obtained by the International Organization of Motor Vehicle Manufacturers (OICA). The results in Figure 10 show that the same pattern arises from what was seen when ratios were compared to GDP. European vehicles rely more heavily on diesel fuel compared to American vehicles, while cars in the US use more gasoline fuel, hence the higher ratios of $XNO_2/\Delta XCO_2$ in European cities and higher ratios of $\Delta XCO/\Delta XCO_2$ in US cities (Ammoura et al., 2014; Hassler et al., 2016). On the other hand, the high ratios of developing cities can be a combination of old car fleets with the large use of coal as anthropogenic fuels which contributes to elevated levels of CO (Clerbaux et al., 2008).

We furthered our analysis by comparing the ratios of $\Delta XCO/\Delta XCO_2$ and $XNO_2/\Delta XCO_2$ to the power plant capacity of each city as shown in Figure 11. The data of power plants were obtained from the Global Database of Power Plants created by the World Resource Institute (WRI) collected from official government data, independent sources around the world, and satellite images. Megacities like Los Angeles, Seoul, and London with large power plant capacities consume large proportions of fossil fuel for energy and show high emission ratios for both $\Delta XCO/\Delta XCO_2$ and $XNO_2/\Delta XCO_2$. Among the developed cities, Los Angeles and Seoul show high ratios of $\Delta XCO/\Delta XCO_2$. This could be attributed to the plumes from coal-fired power generation from industrial units. However, in the case of Los Angeles with a lower capacity of power plants within the city compared to that of Seoul, it is likely that the sources of CO are from other sources like cars more than power

plants. Cities like Mumbai, Kolkata, and Lahore also have an increased ratio of $\Delta XCO/\Delta XCO_2$ more so than $XNO_2/\Delta XCO_2$. These cities are densely populated and are heavily polluted regions of South Asia. In addition, coal is fueling the economic boom of these cities. There has been an increase of more than 50% of coal production and consumption around these cities, as well as large NOx emissions from Indian power plants which have increased by 70% (Duncan et al., 2016). Finally, despite other local influences, cities that are located in basins or surrounded by mountains such as Milan, Tehran, and Daegu continue to show extremely high ratios of $\Delta XCO/\Delta XCO_2$ and $XNO_2/\Delta XCO_2$.

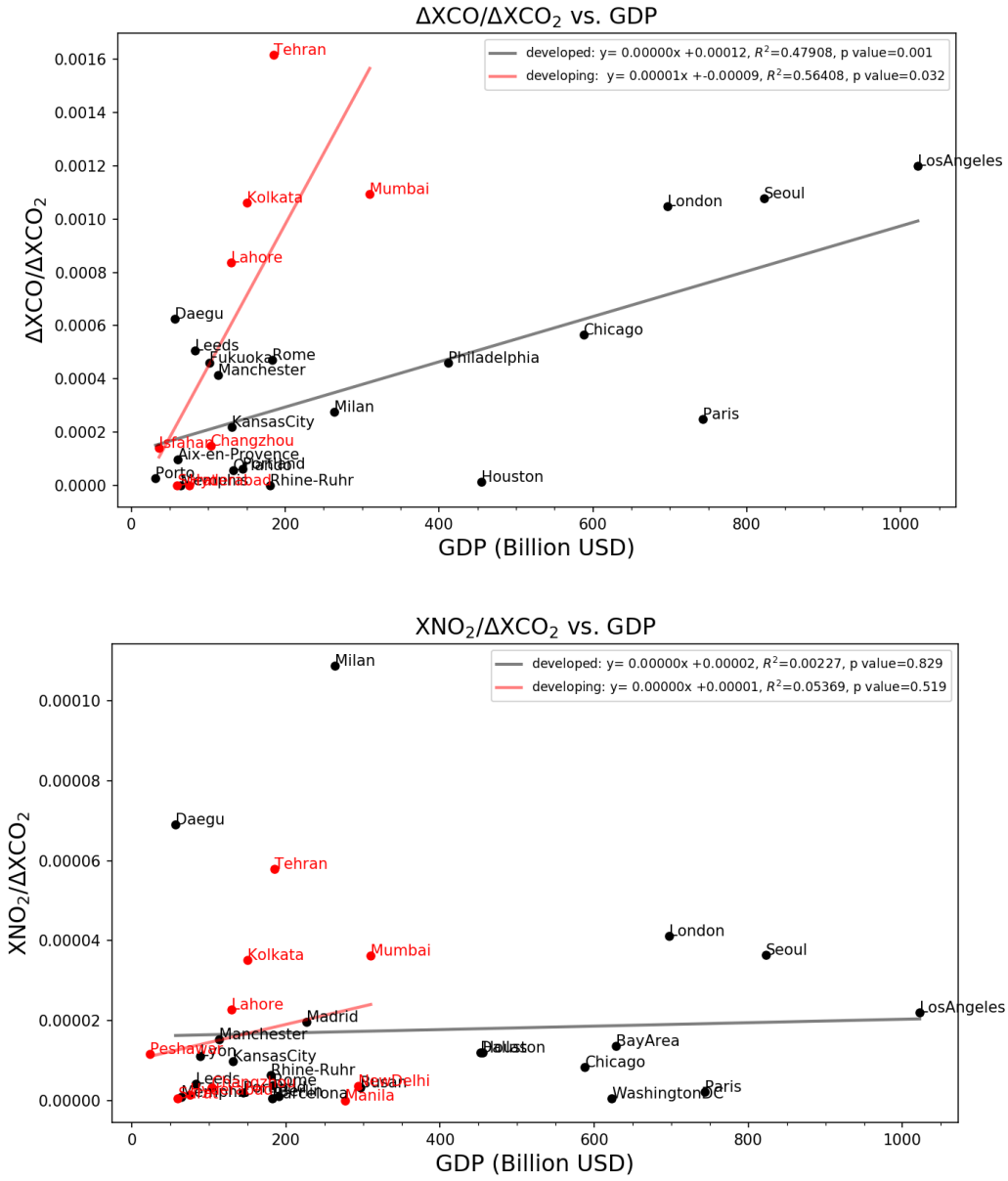

Figure 9. Comparison of $\Delta XCO/\Delta XCO_2$ and $XNO_2/\Delta XCO_2$ to city GDP. Cities classified as 'developed' are marked in black and cities classified as 'developing' are marked in red.

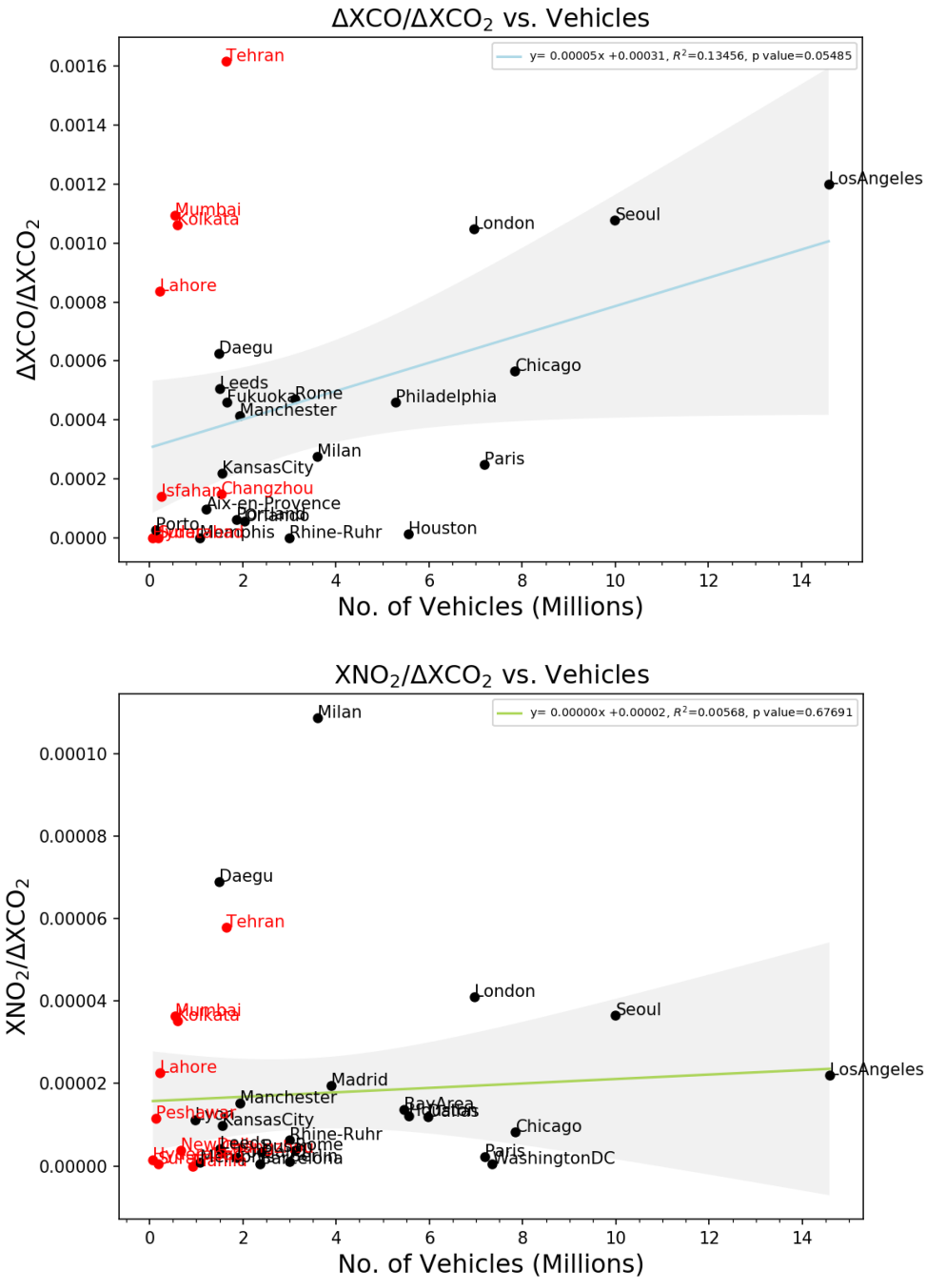

Figure 10. Comparison of $\Delta XCO/\Delta XCO_2$ and $XNO_2/\Delta XCO_2$ to the total number of vehicles in use in the city.

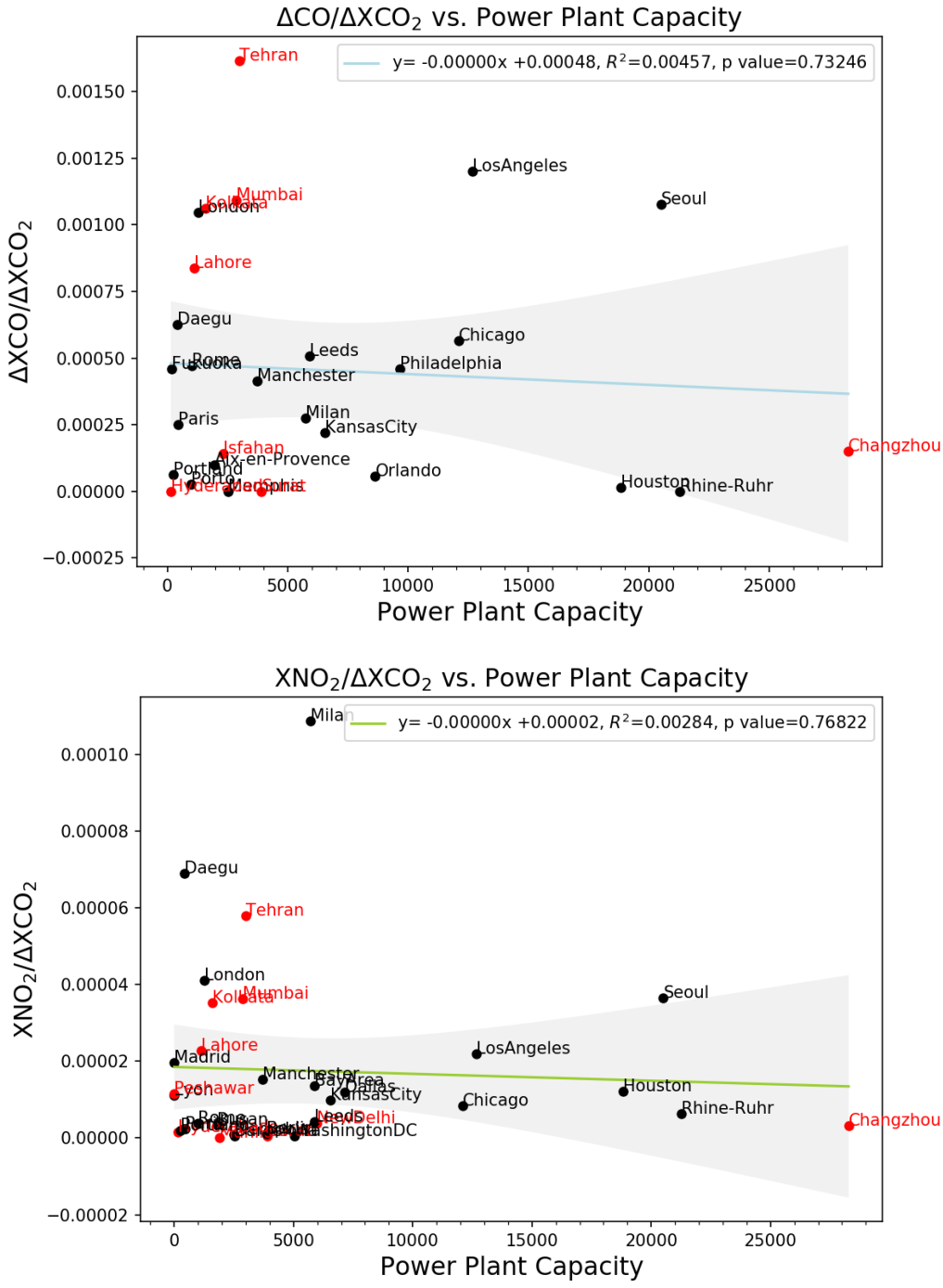

Figure 11. Comparison of $\Delta XCO/\Delta XCO_2$ and $XNO_2/\Delta XCO_2$ to the total power plant capacity within the city.

3.3 Comparison of satellite observations to emission inventory

We extend our analysis to compare our satellite-derived urban enhancements, ΔXCO_2, ΔXCO, and XNO_2, to the Copernicus Atmosphere Monitoring Service (CAMS) Global Emissions Dataset provided by the ECMWF. We used the country totals for the year 2018, which is the data of the most recent year of the emissions dataset. For the comparison of NO_2, we used the NO_X emissions data to compare with satellite-observed XNO_2 enhancements as NO_2 data is not available in the CAMS emissions dataset. Figure 12 is the comparison of the average of the total emissions of the year 2018 to the satellite-observed mean enhancements of all cities in our study. We find that the satellite observed urban enhancements of XNO_2 fit best with the emissions inventory data out of the three gases. The North America region showed the best fit between NO_X emissions and XNO_2, with Europe and Asia placing second and third, respectively.

Reasons why the emissions dataset does not fit well with the satellite-observed urban enhancements can be explored by a closer look at each of the regions. Figure 13 is the same comparison of the CO_2, CO, and NO_X emissions to the satellite-observed ΔXCO_2, ΔXCO, and XNO_2, respectively, made in Figure 12 but plotted separately into regions.

The North America region showed a relatively good fit with CO_2 emissions. This could be the result of more frequent observations and greater sampling of cities in the US from the OCO-2 data. In the CO comparison, North American cities tend to show a higher concentration of ΔXCO compared to CO emissions. In North America, there is a vast amount of forest and crop areas

where frequent forest fires or biomass burning happens. However, the CAMS global anthropogenic emissions dataset for CO does not include emissions from natural fires, which could be a reason why it has not been reflected in the emissions dataset.

Cities in Asia also show a relatively good fit in the CO_2 comparison of emissions data to satellite data with the exception of some cities like Peshawar and Hyderabad. As both cities are in Pakistan, this could be an underreporting of emissions within the country. In the comparison of CO, most cities in Asia show either a higher concentration of ΔXCO compared to the emissions data. As the lifetime of CO can last up to months, the high CO concentration of the city may be transported to the surrounding cities. This would be the case for Seoul which shows a higher concentration of ΔXCO compared to its low CO emission. As the city is located near other polluted cities in East Asia, this could be the result of transport during the wintertime.

Lastly, cities in Europe show a much higher ΔXCO_2 and ΔXCO compared to their respective emissions data. Moreover, geographical influence on atmospheric pollution is also reflected in the comparison between emissions and satellite data. As mentioned in Section 3.1.2, the Po Valley in Northern Italy has a concentration of anthropogenic emissions which also continues to be aggravated by the frequent occurrences of stagnant meteorological conditions caused by the influence of the geographical features of the Alps. In Asia, the same geographical influence is seen in Daegu. The city is surrounded by mountains and located about 80km away from the nearest sea. These geographical features hinder the transport of air pollutants and contain them within the city (Jo & Park, 2005). Like Milan, Daegu consistently shows a higher concentration of ΔXCO_2,

ΔXCO, and XNO_2 compared to its respective emissions data.

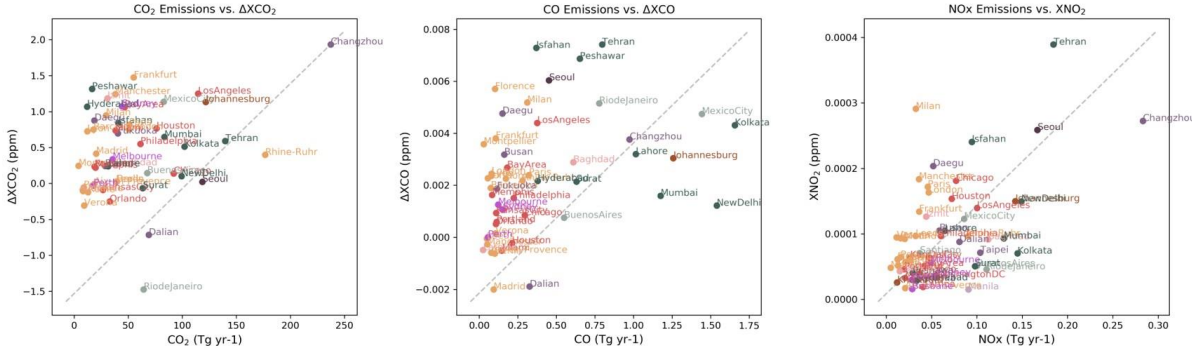

Figure 12. ΔXCO_2, ΔXCO, and XNO_2 of all cities are each compared to CO2, CO, and NOx data of the CAMS Global anthropogenic emissions, respectively.

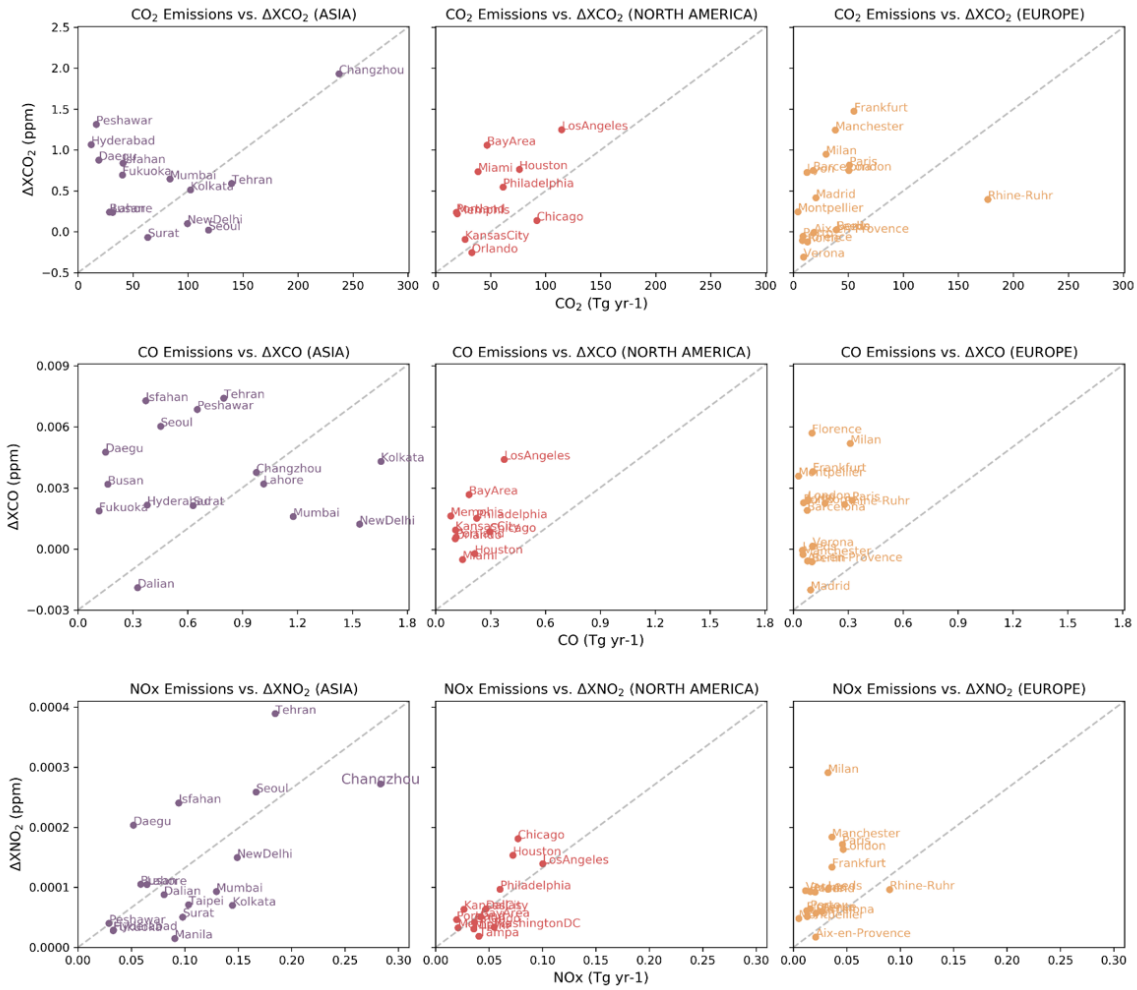

Figure 13. ΔXCO_2, ΔXCO, and XNO_2 of all cities grouped into regions are each compared to CO2, CO, and NOx data of the CAMS Global anthropogenic emissions, respectively.

IV. Discussion and Conclusion

This study demonstrated the use of satellite observations to quantify the urban enhancements of CO_2 and air pollutants CO, and NO_2 using a fair comparison for cities across the globe. This study also showed that regional emission patterns could be characterized using ratios obtained from ΔXCO_2, ΔXCO, and XNO_2. We show that as the concentration of CO_2 increases in the atmosphere, the concentration of air pollutants also increases, leading to a decrease in air quality. The cities in North America fit best with this pattern of relationship out of the three regions compared in our study. The concentration of ΔXCO and XNO_2 per ΔXCO_2, respectively, were mostly from anthropogenic emissions such as home heating and vehicles. However, for ΔXCO, there are also biogenic influences such as natural fires and biomass burning which has been reflected in cities like Rio de Janeiro.

To further analyze the relationship between ΔXCO_2, ΔXCO, and XNO_2, we calculated the $\Delta XCO/\Delta XCO_2$ and $XNO_2/\Delta XCO_2$ for each city. We found that the ratios, $\Delta XCO/\Delta XCO_2$ and $XNO_2/\Delta XCO_2$, were most influenced by its respective air pollutant, which ultimately defines the characteristics of the air quality. When the $\Delta XCO/\Delta XCO_2$ and $XNO_2/\Delta XCO_2$ were compared with city population and GDP, it was found that $\Delta XCO/\Delta XCO_2$ had a positive relationship to city population and GDP, indicating that the size of the city and its economy can act as defining factors of air quality, whereas $XNO_2/\Delta XCO_2$ did not show a strong relationship with either factor. However, the comparison of $\Delta XCO/\Delta XCO_2$ to GDP showed a noticeable difference between cities in Asia and the other two regions of Europe and North America. The higher $\Delta XCO/\Delta XCO_2$ despite their relatively low GDP was a

clear indication of lower combustion efficiency in those cities.

When we divided the cities into 'developed' and 'developing' regions, a distinct pattern was found. Developed cities followed the gradual positive relationship of an increase in the ratios of $\Delta XCO/\Delta XCO_2$ and $XNO_2/\Delta XCO_2$ with the increase of city GDP. However, developing cities facing rapid economic development such as Mumbai, Kolkata, and Lahore were seen to break out of the pattern and reach a high emission ratio that almost matched that of the developed cities. The high emission ratios of $\Delta XCO/\Delta XCO_2$ and $XNO_2/\Delta XCO_2$ in such cities are the results of low combustion efficiency of fossil fuels as well as less stringent pollution control measures.

Finally, we compared our satellite observations of ΔXCO_2, ΔXCO, and XNO_2 to the CAMS Global anthropogenic emissions and found that XNO_2 emission fits best with our observed satellite urban enhancements, while ΔXCO and XCO_2 showed varying patterns within each region. The difference between the emissions dataset and satellite-observed concentrations indicate the influence of transport as well as the uncertainty or underreporting of emissions. In this case, the advantage of satellite observations with uniform global measurements of the atmosphere can be used as a tool for verifying emission inventories. The comparison with emissions data also highlighted the importance of geographical features within or surrounding the city as is the case for Milan, Tehran, and Daegu. These cities are located near mountain ranges or basins where in addition to their high emissions, air pollution gets trapped within the city as a result of meteorological conditions.

Our study which compares CO_2 and air pollutants in cities across the globe with satellites using a uniform method allows us to

characterize air quality as well as different emission patterns that characterize each region. Our findings indicate co-benefit can be achieved where the reduction of CO_2 will result in a reduction of air pollutants CO and NO_2, and vice versa. However, as emission patterns vary by region, it is important to apply different reduction policies and methods according to the varying regional emission patterns. Using the comparison of CO_2 to air pollutants can give clues as to which is the dominant air pollutant that affects the air quality and what factors and sources can affect their concentration.

Despite using only one winter season due to the lack of data availability, our study was able to capture the urban enhancements of cities across the world as well as the distinct features of emission patterns that characterize the regions. However, there were limitations in the sampling size of satellite observations in cities because of the short period of analysis. In addition, unlike the global daily coverage of TROPOMI, OCO-2 makes infrequent visits to cities, and even during those visits, some cities lack data as a result of cloud cover and aerosols, which resulted in the elimination of many cities in our study of places such as China and Russia. With the data of the recently launched OCO-3 satellite and other geostationary Earth observation satellites such as GEMS, TEMPO, and the Sentinels satellites soon to be launched, more in-depth analysis with higher resolution data and a bigger sample of cities can be made in future studies.

References

Ammoura, L., Xueref-Remy, I., Gros, V., Baudic, A., Bonsang, B., Petit, J.-E., Perrussel, O., Bommaire, N., Sciare, J., & Chevallier, F. (2014). Atmospheric measurments of ratios between CO_2 and co-emitted species from traffic: a tunnel study in the Paris megacity, *Atmos. Chem. Phys.*, *14*, 12871-12882, doi:10.5194/acp-14-12871-2014.

Asadollah-Fardi, G. (2008). Air quality management in Tehran. Kitakyushu Initiative Seminar on Urban Air Quality Management, Bangkok, Thailand

Atash, F. (2007). The deterioration of urban environments in developing countries: Mitigating the air pollution crisis in Tehran, Iran. *Cities*, *24*(6), 399-409.

Baker, D. F., Bösch, H., Doney, S. C., O' Brien, D., & Schimel, D. S. (2010). Carbon source/sink information provided by column CO_2 measurements from the Orbiting Carbon Observatory, *Atmos. Chem. Phys.*, *10*, 4145-4165, doi:10.5194/acp-10-4145-2010.

Bares, R., Lin, J. C., Hoch, S. W., Baasandorj, M., Mendoza, D. L., Fasoli, B., ... Stephens, B. B. (2018). The wintertime covariatio of CO_2 and criteria pollutants in an urban valley of the western United States, *JGR Atmospheres*, *123*(5), 2684-2703, https://doi.org/10.1002/2017/JD027917.

Beirle, S., Platt, U., Wenig, M., & Wagner, T. (2003). Weekly cycle of NO 2 by GOME measurements: A signature of anthropogenic sources. *Atmospheric Chemistry and Physics*, *3*(6), 2225-2232.

Bigi, A., Ghermandi, G., & Harrison, R. M. (2012). Analysis of the air pollution climate at a background site in the Po valley. *Journal of Environmental Monitoring*, *14*(2), 552-563.

Briber, B. M., Hutyra L. R., Dunn, A. L., Raciti, S. M., & Munger, J. W. (2013). Variations in atmopsheric CO_2 mixing ratios acrros a Boston, MA urban to rural gradient, *Land*, *2*, 304-327, doi:10.3390/land2030304.

Berezin, E. V., Konovalov, I. B., Ciais, P., Richter, A., Tao, S., Janssesns-Maenhout, G., Beekmann, M., & Schulze, E.-D. (2013). Multiannual changes of CO_2 emissions in China: indirect estimates derived from satellite measurments of tropospheric NO_2 columns, *Atmos Chem. Phys.*, *13*, 9415-9438, doi:10.5194/acp-13-9415-2013.

Bölük, G., & Mert, M. (2014). Fossil & renewable energy consumption, GHGs (greenhouse gases) and economic growth: Evidence from a panel of EU (European Union) countries. *Energy*, *74*, 439-446.

Borsdorff, T., aan de Brugh, J., Pandey, S., Hasekamp, O., Aben, I., Howeling, S., & Landgraf, J. (2019). Carbon monoxide air-pollution on sub-city scales and laong arterial roads detected by the Tropospheric Monitoring Instrument, *Atmos. Chem. Phys. Discuss.*, *19*(6), 3579-3588, doi:10.5194/acp-19-3579-2019.

Ciais, P., Dolman, A. J., Bombelli, A., Duren, R., Peregon, A., Rayner, P. J., … Zehner, C. (2014). Current systematic carbon-cycle observations and the need for implementing a policy-relevant carbon observing system, *Biogeosciences*, *11*, 3547-3602, doi:10.5194/bg-11-3547-2014.

Clerbaux, C., Edwards, D. P., Deeter, M., Emmons, L., Lamarque, J. F., Tie, X. X., … Gille, J. (2008). Carbon monoxide pollution from cities and urban areas observed by the Terra/MOPITT mission, *Geophysical Research Letters*, *35*, L03817, doi:10.1029/2007/GL032300.

Crisp, D., Miller, C. E., & DeCola, P. L. (2008). NASA Orbiting Carbon Observatory: measuring the column averaged carbon dioxide mole fraction from space, *Journal of Applied Remote Sensing*, *2*, 023508, doi:10.117/1.2898457.

Crisp, D., Pollock, H. R., Rosenberg, R., Chapsky, L., Lee, R.A.M., Oyafuso, F.A., … Wunch, D. (2017). The on-orbit performance of the Orbiting Carbon Observatory-2 (OCO-2) instrument and its radiometrically calibrated products, *Atmos. Meas. Tech.*, *10*, 59-81, doi:10.5194/amt-10-59-2017.

Crutzen, P. J., & Andreae, M. O. (1990). Biomass burning in the tropics: Impact on atmospheric chemistry and biogeochemical cycles. *Science*, *250*(4988), 1669-1678.

Duncan, B. N., Lamsal, L. N., Thompson, A. M., Yoshida, Y., Lu, Z., Streets, D. Go., … & Pickering, K. E. (2016). A space-based, high-resolution view of notable changes in urban NOx pollution

around the world (2005–2014). Jo*urnal of Geophysical Research: Atmospheres*, *121*(2), 976–996.

Duren, R. M. & Miller, C. E. (2012). Measuring the carbon emissions of megacities, *Nature Climate Change*, *2*, 560–562, https://doi.org/10.1038/nclimate1629.

Doornink, J., de Vries, J., Voors, R., Dingjan, J., Ording, B., van der Walk, N., … Veefkind, P. (2014). The TROPOMI instrument, last steps towards final integration and testing, *International Conference on Space Optics*, *1056342*, https://doi.org/10.1117/12.2304148.

Eldering, A., O' Dell, C. W., Wennberg, P. O., Crisp, D., Gunson, M. R., Viatte, C., … Yoshimizu, J. (2017a). The Orbiting Carbon Observatory–2: first 18 months of science data products, *Atmos. Meas. Tech*, *10*, 549–563, doi:10.5194/amt–10–549–2017.

Eldering, A., Wennberg, P. O., Crisp, D., Schimel, D. S., Gunson, M. R., Chatterjee, A., … Weir, B. (2017b). The Orbiting Carbon Observatory–2 early science investigations of regional carbon dioxide fluxes, *Science*, *358*(6360), eaam5745, doi:10.11256/science.aam5745.

Granier, C., Darras, S., van der Gon, H. D., Jana, D., Elguindi, N., Bo, G., ... & Liousse, C. (2019). The Copernicus Atmosphere Monitoring Service global and regional emissions (April 2019 version).

Hakkarainen, J., Ialongo, I., & Tamminen, J. (2016). Direct space-based observations of anthropogenic CO_2 emission areas from OCO-2, *Geophysical Research Letters*, *43*(21), 11400-11406, https://doi.org/10.1002/2016GL070885.

Hakkarainen, J., Ialongo, I., Maksyutov, S., & Crisp, D. (2019). Analysis of four years of global XCO_2 anomalies as seen by Orbiting Carbon Observatory-2, *Remote Sensing*, *11*, 850, doi:10.3390/rs11070850.

Hassani, A., & Hosseini, V. (2016). An assessment of gasoline motorcycle emissions performance and understanding their contribution to Tehran air pollution. *Transportation research part D: Transport and environment*, *47*, 1-12.

Hassler, B., McDonald, B. C., Frost, G. J., Borbon, A., Carslaw, D. C., Civerolo, K., ... & Pollack, I. B. (2016). Analysis of long-term observations of NOx and CO in megacities and application to constraining emissions inventories. *Geophysical Research Letters*, *43*(18), 9920-9930.

Hilboll, A., Richter, A., & Burrows, J. P. (2013). Long-term changes of tropospheric NO2 over megacities derived from multiple satellite instruments. *Atmospheric Chemistry and Physics*, *13*(8), 4145.

Hutyra, L. R., Duren, R., Gurney, K. R., Grimm, N., Kort, E. A., Larson, E. & Shrestha, G. (2014). Urbanization and the carbon cycle: current capabilities and research outlook from the natural sciences perspective, *Earth's Future*, *2*(10), 473-495, https://doi.org/10.1002/2014EF000255.

Jo, W. K., & Park, J. H. (2005). Characteristics of roadside air pollution in Korean metropolitan city (Daegu) over last 5 to 6 years: temporal variations, standard exceedances, and dependence on meteorological conditions. *Chemosphere*, *59*(11), 1557-1573.

Koplitz, S. N., Jacob, D. J., Sulprizio, M. P., Myllyvirta, L., & Reid, C. (2017). Burden of disease from rising coal-fired power plant emissions in Southeast Asia. *Environmental science & technology*, *51*(3), 1467-1476.

Kort, E. A., Frankenberg, C., Miller, C. E., & Oda, T. (2012). Space-based observations of megacity carbon dioxide, *Geophysical Research Letters*, *39*(17), 1-5, https://doi.org/10.1029/2012GL052738.

Kroktov, N. A., McLinden, C. A., Li, C., Lamsal, L. N., Celarier, E. A., Marchenko, S. V., … Streets, D. G., (2016). Aura OMI observations of regional SO_2 and NO_2 pollution changes from 2005 to 2016, *Atmos. Chem. Phys.*, *16,* 4605-4629, doi:10.5194/acp-16-4605-2016.

Labzovskii, L. D., Jeong, S. J., & Parazoo, N. C. (2019). Working towards confident spaceborne monitoring of carbon emissions from cities using Orbiting Carbon Observatory-2, *Remote Sensing of Environment*, *233*, 111359, https://doi.org/10.1016/j.rse.2019.111359.

Levine, J. S. (1994). Biomass burning and the production of greenhouse gases. *Climate biosphere interaction: biogenic*

emissions and environmental effects of climate change. John Wiley, New York, New York, USA, 139-160.

Molina, L. T., Molina, M. J., Slott, R. S., Kolb, C. E., Gbor, P. K., Meng, F., …Gertler, A. W. (2004). Air quality in selected megacities, *Journal of the Air & Waste Management Association*, *54*(12), 1-73, doi:10.1080/10473289.2004.10471015.

Moran, D., Kanemoto, K., Jiborn, M., Wood, R., Többen, J., & Seto, K.C. (2018). Carbon footprints of 13000 cities, *Environ. Res. Lett., 13*, 064041, https://doi.org/10.1088/1748-9326/aac72a.

O' Dell, C.W., Eldering, A., Wennberg, P.O., Crisp, D., Gunson, M.R., Fisher, B.; Frankenberg, C., … Velazco, A. (2018). Improved retrievals of carbon dioxide from Orbiting Carbon Observatory-2 with the version 8 ACOS algorithm, *Atmos. Meas. Tech., 11*, 6539-6576, https://doi.org/10.5194/amt-11-6539-2018.

Parrish, D. D. & Zhu, T. (2009). Clean air for megacities. *Science*, *326*, 674-675, doi:10.1126/science.1176064.

Reuter, M., Buchwitz, M., Hilboll, A., Richter, A., Schneising, O., Hilker, M., … Burrows, J. P. (2014). Decreasing emissions of NO_X relative to CO_2 in East Asia inferred from satellite observations, *Nature Geoscience*, *7*(11), 792-795, doi:10.1038/ngeo2257.

Reuter, M., Buchwitz, M., Schneising, O., Krautwurst, S., O' Dell, C. W., Richter, A., Bovensmann, H., and Burrows, J. P. (2019). Towards monitoring localized CO2 emissions from space: co-located regional CO2 and NO2 enhancements observed by the

OCO-2 and S5P satellites, *Atmos. Chem. Phys.*, *19*, 9371-9383, https://doi.org/10.5194/acp-19-9371-2019.

Rhys-Tyler, G. A., Legassick, W., & Bell, M. C. (2011). The significance of vehicle emissions standards for levels of exhaust pollution from light vehicles in an urban area. *Atmospheric Environment*, *45*(19), 3286-3293.

Richter, A., Burrows, J. P., Nüß, H., Granier, C., and Niemeier, U. (2005). Increase in tropospheric nitrogen dioxide over China observed from space, *Nature*, *437*, 129-132, doi:10.1038/nature04092.

Sakugawa, H., & Kaplan, I. R. (1997). Radio and stable-isotope measurements of atmospheric carbon monoxide in Los Angeles. *Geochemical Journal*, *31*(2), 75-83.

Seibert, P., Kromp-Kolb, H., Kasper, A., Kalina, M., Puxbaum, H., Jost, D. T., ... & Baltensperger, U. (1998). Transport of polluted boundary layer air from the Po Valley to high-alpine sites. *Atmospheric Environment*, *32*(23), 3953-3965.

Schneider, A., Friedl, M. A., & Potere, D. (2009). A new map of global urban extent from MODIS satellite data, *Environ. Res. Lett.*, *4*, 044003, doi:10.1088/1748-9326/4/4/044003.

Schneider, P., Lahoz, W. A., & van der A, R. (2015). Recent satellite-based trends of tropospheric nitrogen dioxide over large urban agglomerations worldwide, *Atmos. Chem. Phys.*, *15*, 1205-1220, doi:10.5194/acp-15-1205-2015.

Silva, S. J. & Arellano, A. F. (2017). Characterizing regional-scale combustion using satellite retrievals of CO, NO_2 and CO_2, *Remote Sensing*, *9*(7), 744, doi:10.3390/rs9070744.

Silva, S. J., Arellano, A. F., & Worden, H. M. (2013). Toward anthropogenic combustion emission constraints from space-based analysis of urban CO_2/CO sensitivity, *Geophysical Research Letters*, *40*, 4971-4976, doi:10.1002/grl.50954.

Souri, A. H., Choi, Y., Jeon, W., Li, X., Pan, S., Diao, L., & Westenbarger, D. A. (2016). Constraining NO_X emissions using satellite NO_2 measurements during 2013 DISCOVER-AQ Texas campaign, *Atmospheric Environment*, *131*, 371-381, doi:10.1016/j.atmosenv.2016.02.020.

Tariq, S., & Ali, M. (2015). Tropospheric NO2 trends over South Asia during the last decade (2004-2014) using OMI data. *Advances in Meteorology*, *2015*.

Turnbull, J. C., Tans, P. P., Lehman, S. J., Baker, D., Conway, T. J., Chung, Y. S., ... & Zhou, L. X. (2011). Atmospheric observations of carbon monoxide and fossil fuel CO2 emissions from East Asia. *Journal of Geophysical Research: Atmospheres*, *116*(D24).

Veefkind, J., Aben, I., McMullan, K., Förster, H., de Vries, J., Otter, G., ... Levelt, P. F. (2012). TROPOMI on the ESA Sentinel-5 Precursor: A GMES mission for global observations of the atmospheric composition for climate, air quality and ozone layer applications, *Remote Sensing of Environment, 120,* 70-83, doi:10.1016/j.rse.2011.09.027.

Worden, H. M., Deeter, M. N., Edwards, D. P., Gille, J. C., Drummond, J. R., & Nédélec, P. (2010). Observations of near-surface carbon monoxide from space using MOPITT multispectral retrievals, *Journal of Geophysical Research*, *115*, D18314, doi:10.1029/2010JD014242.

Wunch, D., Wennberg, P. O., Toon, G. C., Keppel-Aleks, G., & Yavin, Y. G. (2009). Emissions of greenhouse gases from a North American megacity, *Geophysical Research Letters*, *36*(15), 1-5, https://doi.org/10.1029/2009GL039825.

국문 초록

인공위성 관측 자료 기반으로 CO_2 및 대기오염물질의 상관성을 이용한 도시의 배출 특성 분석

박하영
환경계획학과 환경관리전공
서울대학교 환경대학원

도시는 인위적인 이산화탄소(CO_2) 배출의 70% 이상을 차지하고 있으며 대기 오염의 큰 원천이다. 전 세계적으로 도시화가 증가함에 따라 도시는 급속도로 성장하고 있으며, 도시 내 인간의 활동과 에너지 소비량의 증가에 따라 대기질에 큰 영향을 미치는 이산화탄소와 대기 오염물질의 배출도 함께 증가하였다. 본 연구는 2018년 12월부터 2019년 3월까지 NASA의 Orbiting Carbon Observatory-2 (OCO-2)에서 관측된 CO_2와 ESA의 Sentinel-5 Precursor TROPOMI(S-5P TROPOMI)에서 관측된 대기오염물질 CO 및 NO_2의 도시 증가량을 모니터링 할 수 있는 가능성을 탐구한다. 인공위성 관측자료를 이용하여 각 도시에 따른 ΔXCO_2, ΔXCO, XNO_2의 도시 증가량과 $\Delta XCO/\Delta XCO_2$ 및 $XNO_2/\Delta XCO_2$의 도시 증가량 비율을 분석하여 CO_2와 대기오염물질과의 관계뿐만 아니라 도시의 배출 패턴도 함께 관찰한다.

본 연구 결과에서 ΔXCO_2가 ΔXCO 및 XNO_2와 양의 관계를 가졌고, 이는 CO_2의 증가가 대기오염물질의 증가로 이어질 수 있음을 보여주었다. 그러나 도시를 지역별로 분류할 때 서로 다른 패턴을 보였다. 아시아 지역의 도시들은 CO_2 대비 대기오염물질의 농도가 가장 높았고, 미국 지역의 도시들은 CO_2와 대기오염물질 간에 가장 높은 양의 상관성을 보였다. $\Delta XCO/\Delta XCO_2$와 $XNO_2/\Delta XCO_2$의 비교는 지역에 따라 뚜렷한

배출 패턴을 보인다. $\Delta XCO/\Delta XCO_2$와 $XNO_2/\Delta XCO_2$를 도시 인구 및 GDP와 비교했을 때 모두 양의 상관성이 있었으며, 이는 도시 규모와 도시의 경제 규모가 대기질의 요인을 정의하는 역할을 할 수 있음을 나타냈다. 더 나아가 도시들을 해당 나라의 경제적 수준에 따라 'developed' 과 'devleoping' 으로 나누었을 때 또 다른 패턴이 발견되었다. 선진국 도시들은 도시 GDP의 증가에 따라 $\Delta XCO/\Delta XCO_2$와 $XNO_2/\Delta XCO_2$의 비율은 점진적인 양의 관계를 따랐지만, 뭄바이, 콜카타, 라호르와 같은 급속한 경제발전을 하는 개발도상국 도시들은 그 패턴에서 벗어나 선진국 도시들과 거의 일치하는 높은 증가량 비율을 보였다. 이러한 도시에서 $\Delta XCO/\Delta XCO_2$ 및 $XNO_2/\Delta XCO2$의 높은 증가량 비율은 화석 연료의 낮은 연소 효율에 더불어 엄격하지 않은 오염 통제 조치의 결과물이다.

마지막으로, 인공위성으로 관측된 ΔXCO_2, ΔXCO, XNO_2를 CAMS 글로벌 인위적 배출량 데이터와 함께 비교하였다. 그 결과, XNO_2 배출량이 위성으로 관측된 도시 증가량과 가장 잘 맞았지만, ΔXCO와 ΔXCO_2는 각 지역 내에서 다양한 패턴을 보였다. CAMS 배출량 데이터와 위성으로 관측된 농도 간의 차이는 배출량 불확실성, 정확하지 않은 배출량 보고, 대기 중 운송 등의 영향을 나타낸다. 배출량 데이터와의 비교는 밀라노, 테헤란, 대구와 같은 도시의 경우처럼 도시를 둘러싼 지리적 특징의 중요성을 부각했다. 이런 도시들은 산맥 근처나 분지에 있으며, 높은 배출량 외에도 지리적 특징과 함께 기상 조건의 결과로 대기 오염이 도시 안에 갇히게 된다.

본 연구는 전 세계 도시의 CO_2와 대기오염물질을 인공위성을 사용해 동일한 방법으로 비교하여 각 지역의 배출 특성과 배출 패턴을 분석하였다. 본 연구의 결과는 CO_2의 감소가 대기오염물질인 CO와 NO_2를 감소시키는 결과를 가져오는 co-benefit을 얻을 수 있다는 것을 시사한다. 단, 지역별로 배출 패턴과 특성이 다르기 때문에 지역별 배출

특성에 따라 다른 감축 정책과 방법을 적용하는 것이 중요하다. 본 연구는 대기오염물질과 CO_2의 비교를 통해 대기질에 영향을 미치는 지배적인 대기오염물질과 그 농도에 영향을 미칠 수 있는 요인과 배출원이 무엇인지에 대한 실마리를 얻을 수 있다는 것을 보여준다.

주요어 : CO_2, CO, NO_2, 도시 증가량, 비율, 배출 패턴
학 번 : 2018-24455